Valeology: International Journal of Medical Anthropology and Bioethics
(ISSN 2995-4924) VOLUME 02 ISSUE 12, 2024

AN AMMONIA GAS SENSOR BUILT WITH ZNO NANORODS: CHARACTERIZATION

Mohammed N Ali, Faris Hassan Taha
University of Al-Kitab, Engineering Technical College, Dept. of Biomedical Instrumentation Engineering

Rusul Taha Hussain Abd
Salahaddin Education Directorate / Tikrit Department

Muhannad Khalil Ibrahim
University of Al-Kitab, Engineering Technical College, Dept. Cyber Security

Abstract:

Drop casting was used to create nano-rod Zinc oxide (ZnO). The next step was employing ZnO nanorod to create thin films using the Drop casting method on a glass substrate. These films were dried and burned for two hours in an environment of air at 400oC. Using the SEM, EDAX, and XRD techniques, respectively, the morphological, compositional, and structural characteristics of the ZnO nanorod were examined. Nanorod ZnO film samples' chemical composition varies with firing temperature and exhibits non-stoichiometric behaviors. An XRD analysis showed that hexagonal ZnO sheets with a hexagonal wurtzite structure had formed. I investigated the ZnO flim coatings on nanorods NH3 sensing capabilities at a temperature of 50 °C.

Keywords: Nano-rod ZnO; gas sensitivity; NH_3.

Introduction

INTRODUCTION

Gas sensors need to be used in factories or petrochemical plants. Use these gas sensors to monitor the environment as an important early warning device to protect health and monitor pollutants such as NOx, SOx, ammonia (NH3), and H2S. With over 100 million tons produced annually, NH3 is one of the most leading chemicals [1]. Besides being used in semiconductors, it is also used in many of the world's food industries, the refrigeration industry, and clinical medicine. [2]. An irritating gas

to the eyes and upper respiratory system, NH_3 has no color and a strong odor. It has an impact on human health in low quantities. Thus, NH3 detection becomes substantially crucial. Over the period of about ten years, a number of major researches were conducted on common air quality inspector stations and miniature gas sensors using infrared dots, catalytic beads, photoionization, and metal oxide semiconducting (MOS) sensors. [3] Recently, a hybrid plasmonic waveguide with a polarization-insensitive design that can detect methane gas [4] and acetylene utilizing $SmFeO_3$ material has also been described. [5]. Gas sensors, however, need to be miniaturized, sensitive, and have lower power and cost for applications that protect human health while in motion. Because of their tiny size, low cost, and compatibility with silicon-based microelectronic devices, MOS sensors have received a great deal of research attention. Microelectromechanical systems (MEMS) using semiconductor sensors are suited for wearable applications because they can be easily integrated into consumer electronics. SnO_2, ZnO, CuO, La_2O_3, CeO, and TiO_2 are some of the MOS components that make up this list. [11]. With a 3.12 electron volt bandgap at ambient temperature and a 60 electron volt exciton binding energy, ZnO is a chemically and thermally durable n-type MOS that is frequently employed in photodetectors, pH sensors, and devices that detect poisonous and flammable gases [12]. The sensitivity and power consumption of MOS gas sensors keep getting better. High-performance sensors such as nanostructured ones would have the highest response as opposed to body membrane and thin film sensors, owing to the reason that they have a great aspect ratio and high surface area to volume ratio so that sensors could be made more sensitive with nanostructures like nanowires, nanoparticles, and nanotubes [7]. Further, gas sensors need to be able to identify harmful gases at room temperature (25 °C) to save power. Wang et al. have reported a gas sensor that operates at room temperature. [14]. A room-temperature operating H_2S gas sensor with aligned ZnO nanorods and flower-like structures was described by Irajizad et al. [15]. The sensor has responded to 581 for five ppm H2S. Dong et al. described room temperature ZnO nanorods NH3 gas sensor; the results show that the sensitivity is about eight at 500 ppm NH3 [16]. The present study gives an ultrasonic wave grinding technique to produce ZnO nanorods (ZnO-NRs), which end up being integrated into the MEMS structure to produce ZnO-NRs/MEMS NH3 room temperature gas sensor. Characteristics of the ZnO-NRs and fabrication of the sensor are discussed. It is also ascertained how ZnO NRs sense NH3 gas at room temperatura conditions.

MATERIALS AND METHODS

The readiness of nano-pole ZnO was finished from the drop projecting strategy at room temperature on glass substrates. (10mM) arrangement of zinc home (Zn(C4H5).6H2O) for getting ready zinc oxide (ZnO) independently breaks down in (50 Ml) of ethanol with consistent blending for (30 min). Drop projecting was utilized to the blend of the ZnO nanostructure seed layer; the bead was change with an area of substrate by (20µL/cm2). Similar rehashing was rehashed multiple times, and after each step, it was flushed with ethanol at the point when the substrate covered with ZnO seed layer is warmed at (400oC) to get solid adherence and arrangement of ZnO nanorod. Disintegrate (25mM) arrangement of zinc nitrate-Zn(NO3)2 .6H2O getting ready zinc oxide (ZnO) and break down independently in (50 mL) of water with nonstop mixing at for (30) min(25mM) arrangement of Hexamethylenetetramine (HMTA) (C6H12N4) in (50 mL) of water was broken up with consistent blending at for (30 min). Arrangements of stage 3 and stage 4 were blending in with constant mixing at for (30min). The last arrangement was put into a Teflon-lined tempered steel autoclave. This autoclave is fixed right away and kept at (90) oC for (2h) in a computerized temperature-controlled stove substrate development ZnO nanorod where An Energy Dispersive Spectrometer was utilized to look at the piece of tests of ZnO thick film (JOELJED 6360 LA). Utilizing the Taylor-Hobson (Taly-step UK) framework, the thickness of the ZnO thick movies was estimated. The movies' thicknesses were reliably somewhere in the range of 20 and 22 mm. In an environment with differing temperatures, the D.C. Opposition of the movies was resolved utilizing the half-span strategy. The static gas-detecting gadget was utilized for the gas-detecting studies,

which were directed in a run-of-the-mill research facility setting. Thick film gas reaction was examined in a test get-together.

$$S = \frac{R_a - R_g}{R_a} \quad -----(1)$$

$$D_{av} = \frac{K\lambda}{\beta \cos\theta} \ldots\ldots\ldots (2)$$

RESULTS AND DISCUSSION

The components of the 400°C-fired films are listed in Table 1. Before the Au metal is sputtered, the EDX of the ZnO film produced using the Drop casting technique process is displayed. Only the peaks of zinc (Zn) and oxygen (O), whose respective contributions to the total atomic percentages are 22.4 and 77.6%, are visible in the graph. The sample's pure ZnO composition can also be detected in the EDS spectrum shown in Fig. This conclusion leads to nonstoichiometry in the solid and agrees with the FE-SEM and X-ray diffraction investigations. As can be seen from the spectrum, samples obtained using the thermal evaporation methodology contain more zinc and oxygen than samples prepared using other techniques. This results

Table-1: Composition of the ZnO by by Drop casting method films at 400°C.

Element	Wt%	At%
Zn	77.6	0.5
O	22.4	0.5

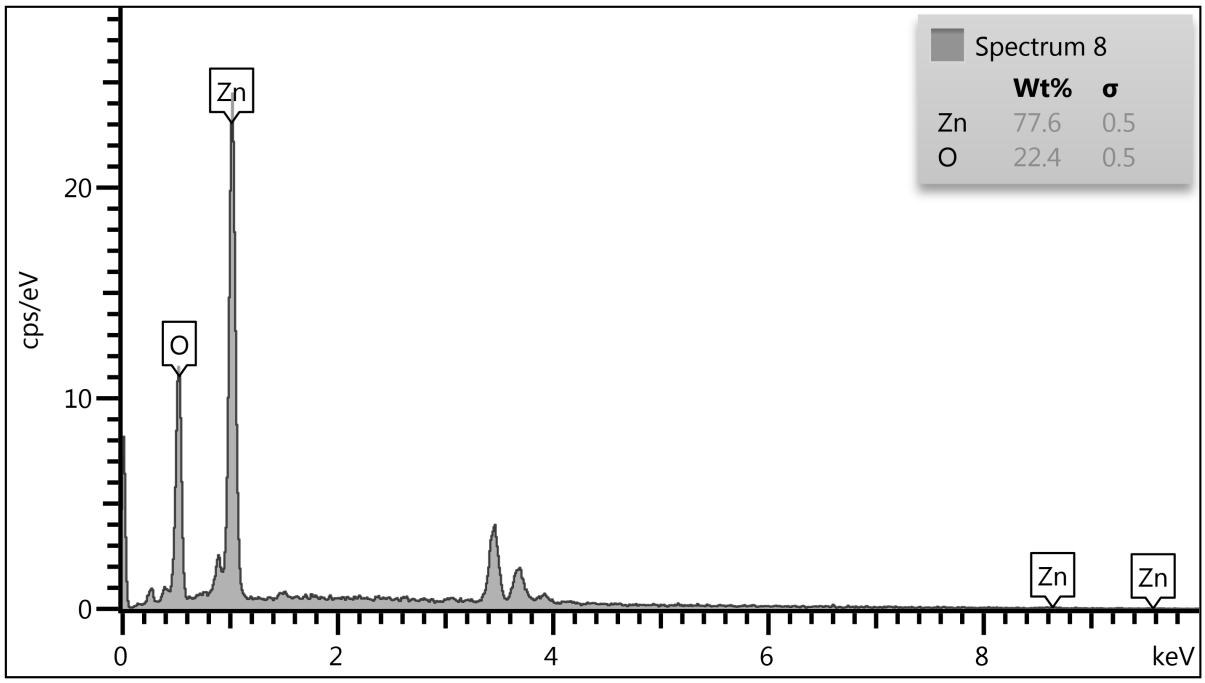

Figure (1): EDS of ZnO thin film prepared by Drop casting method

The X-R diffraction examples of a splash-covered nano-bar ZnO meager film on a glass substrate are displayed in Fig. 2. Various pinnacles of stage ZnO show up in the XRD design. It has been seen that [101] reflections with the greatest power at 2θ = 36.17o for all movie tests propose significant stacking of the plane along the c-pivot, showing that the ZnO movie had a leaned toward

direction that way. It is feasible to recognize the ZnO diffraction tops for the gem directions of (110), (101), (200), (200), and (310). The assessed values concur with the JCPDS information card Number 21-1486, which addresses the typical interplaner separating. This exhibits unequivocally that polycrystalline is the idea of the ZnO film structure. Other than ZnO tops, no other contamination top is apparent, showing creation.

Fig.:2. X-ray Diffraction (XRD) analysis of ZnO Seed Layer thin films

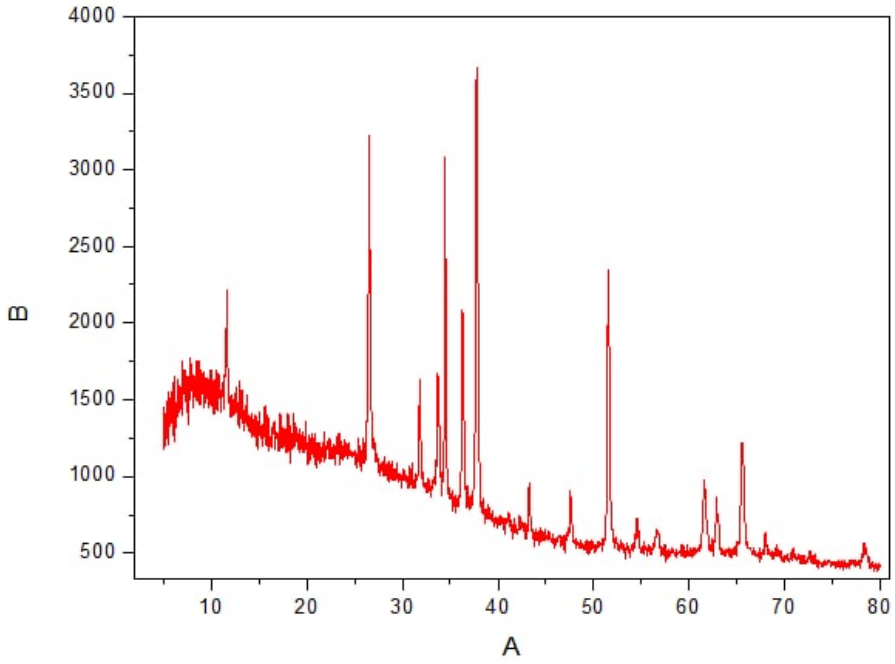

To examine the surface morphology of deposited films, the field emission scanning electron microscope is a helpful tool. FESEM scans reveal a porous, wafer-like structure. This is due to the film's porosity as it was deposited at ambient temperature. Figure 3 displays FESEM images of thin films of nanostructured ZnO nanorods heated to 400 oC in the.

Microstructure characterization was done using FESEM. The images have a rod-type nanostructure that is porous, though some intragranular porosity still remains. The film fired at 400°C has a good adherence characteristic and is thus used for gas sensing applications.

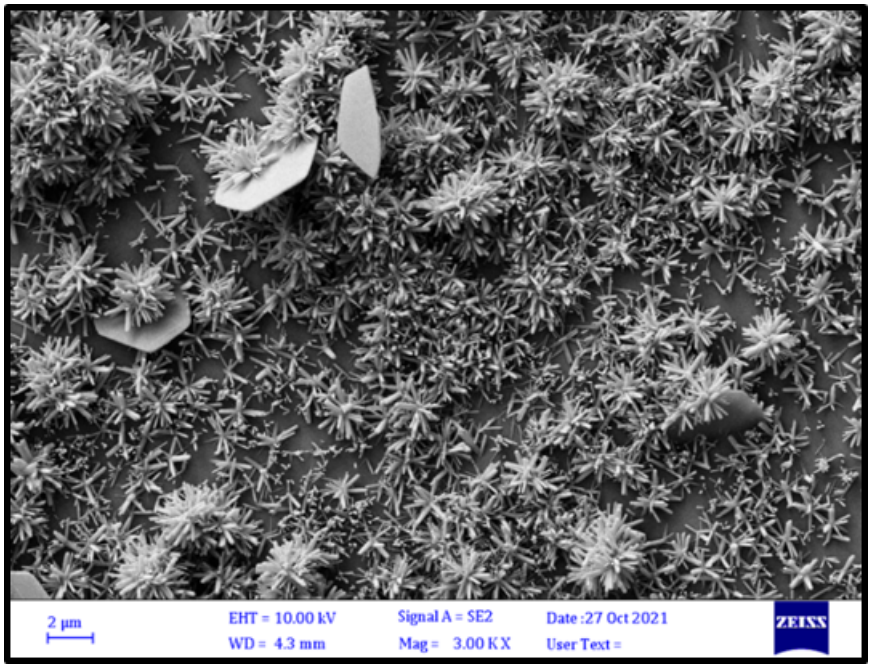

Figure-3 FESEM images of ZnO nanorod film prepared by a Drop coating.

As shown in Figure 4, the response of pure ZnO burned at 400oC with respect to 500 ppm NH3 gas has a variation in operating temperature. Between 25 and 50oC, The response of pure ZnO burned at 400ºC to 500 ppm NH_3 gas varies with operation temperature, as shown in Figure 4. From 25 to 50ºC, the gas reaction rises with temperature and then falls as the temperature rises more. At 50ºC, pure ZnO reacts with NH_3 gas at a ratio of 97.77. In the current study, the ZnO film was given 15 minutes to settle at an operating temperature before being exposed to NH_3, and the stabilized resistance was taken as Ra. The altered resistance was calculated as Rg after the film had been exposed to the NH_3 gas. A reducing gas is NH_3. It reacts with the film's surface oxygen ions. The quantity of free carriers rises as the film is reduced. Consequently, the resistivity of

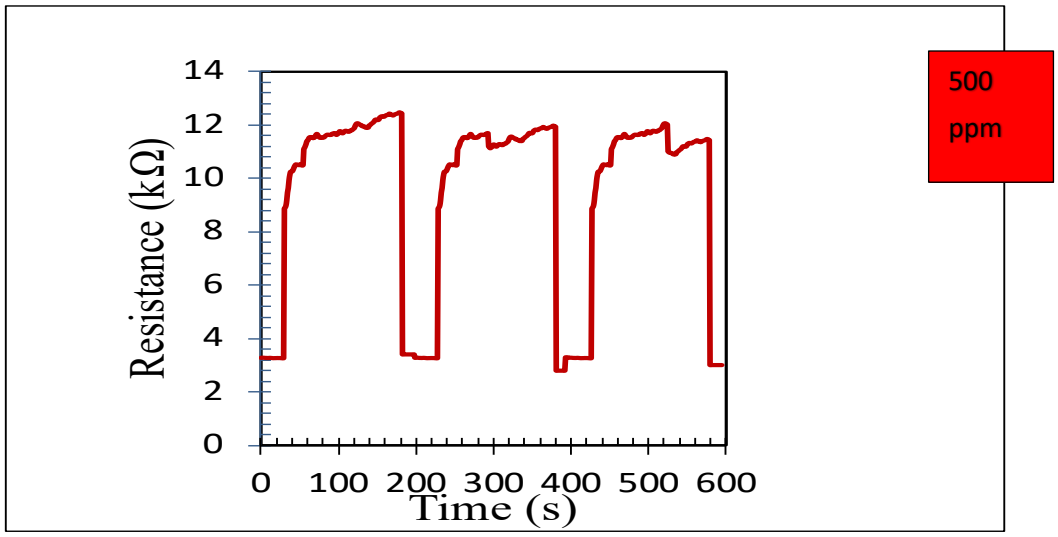

Fig.4 Variation of response with operating temperature for NH3 gas at 500 ppm.

Figure 5 shows the fluctuation in gas response of the ZnO film sample with NH_3 gas concentration at 50ºC temperature. Different NH_3 gas concentrations were used to expose this film. The sensitivity levels were seen to steadily rise as gas concentrations rose up to 500 ppm**.**

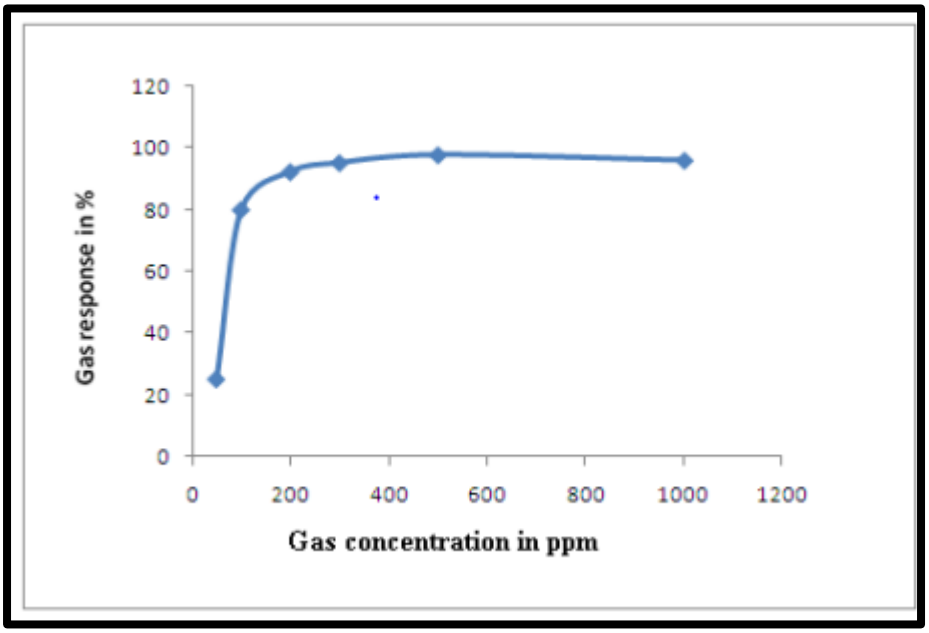

Fig.4. Variation of gas response with gas concentration.

Figure 5 demonstrates that the ZnO sample responds to NH_3 (500 ppm) at its greatest level at 50 degrees Celsius. The sample displayed the highest selectivity for NH_3 in comparison to all other tested gases, including NO_2 LPG. CO_2, H_2S, and ethanol vapors.

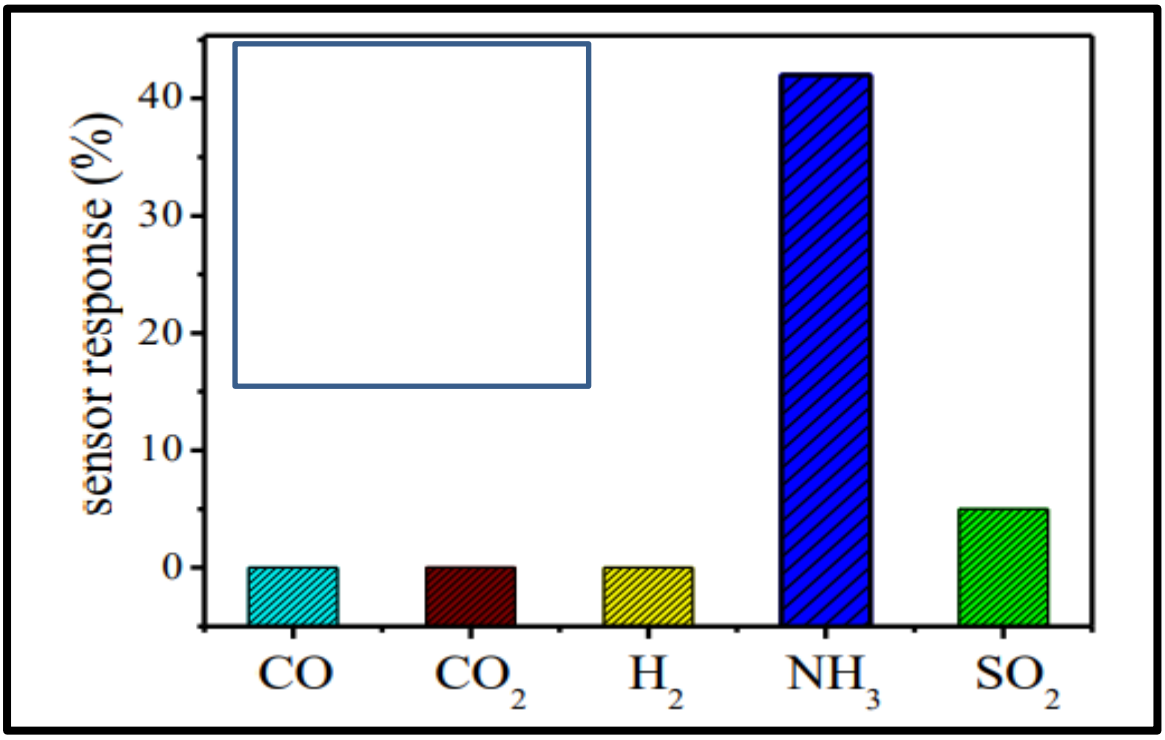

Fig. 5 Selectivity of ZnO sample for various gases

Figure 6 shows the ZnO film sample's reaction and recovery times. The response time to 500 ppm of NH_3 was only 14 seconds, while the recovery time was only 25 seconds. The speedy response could be the result of accelerated gas oxidation. Because of its high volatility, it reacts quickly and returns quickly to its initial chemical form.

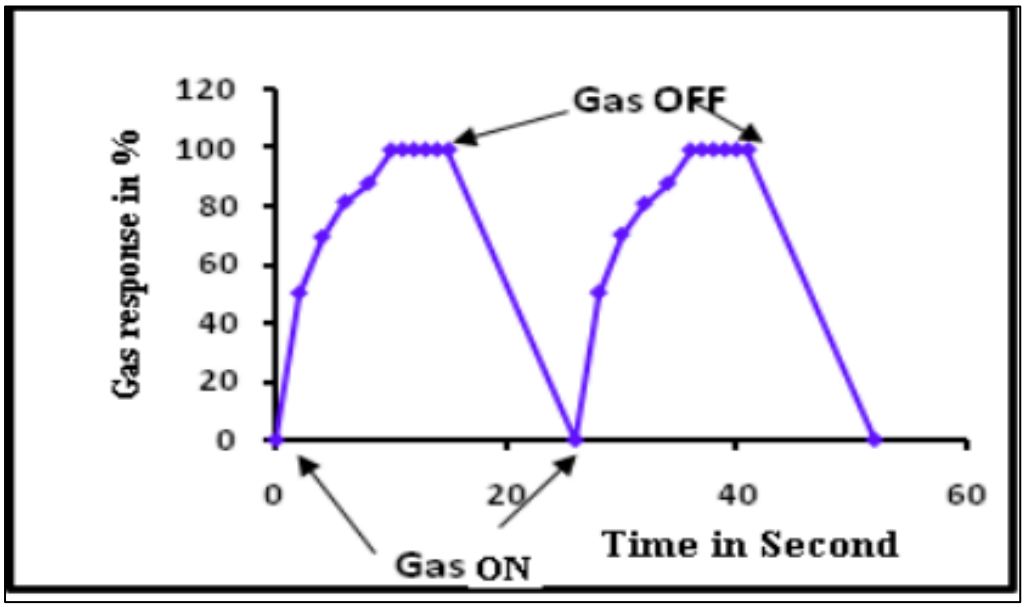

Fig. 6 Response and recovery of ZnO sample

CONCLUSION

Successful Nano-rod zinc oxide has been synthesized by Drop casting methods. The resulting ZnO nanorods will be used to fabricate thin films on a glass substrate using standard screen printing techniques. Nanopowders ZnO screen printed thick film showed good adhesive property to the glass substrate by employing a simple, cheap method and possible uses of the ZnO films for NH3 gas sensing, while thin-film fired at 400ºC gave good sensing performance toward NH3 at a 50C temperature.

REFERENCES

1. K. L. Chopra, S. Major, and D. K. Pandya, Thin Solid Films, 1983, Vol. 102, Iss.1, 1-96.
2. A. P. Roth and D. F. Williams, J. Electrochem. Soc. 1981, Vol.128, Issue 12, 2684-2686.
3. Ohya Yutaka, Saiki Hisao, Tanaka Toshimasa and Takahashi Yasutaka, J. Am. Ceram. Soc., 1996, Vol. 79, 825
4. Joseph Benny, K G Gopchandran, P K Manoj, J T Abraham, Koshy Peter and V K Vaidyan, Indian J. Phys., 1998, A72 99
5. Berhanu D, Boyle D S, Govender K, and O'Brien P 2003 J. Mater. Sci.: Mater. Elect. 14 579
6. Sun-Ki Min, Rajaram S. Mane, Oh-Shim Joo, T. Ganesh, Byung Won Cho, Sung-Hwan Han, Current Applied Physics, In Press, 2008.
7. A. P. Alivisatos, Science New series, 1996, Vol. 271, No 5251, 933-937.
8. W.J.E. Beek, M.M. Wienk, R.A.J. Janssen, Adv. Mater., 2004, 16, , 1009.
9. W.J.E. Beek, M.M. Wienk, M.K. Emerink, X. Yang, R.A.J. Janssen, J. Phys. Chem. B, 2005, 109, 9505.
10. Y. Xia, P. Yang, Y. Sun, Y.Wu, B. Mare, B. Gates, Y. Yin, F. Kim, H. Yan, Adv. Mater. 2003, 15, 323.
11. Z.M. Jarzebzki, in: R.B. Pamplin (Ed.), Pergamon Press, Oxford, 1973. Q1
12. M.H. Huang, Y.Wu, H. Feick, N. Tran, E.Weber, P. Yang, Adv. Mater. 2001, 13, 113.

13. D. J. Goyal, C. Agashe, M. G. Takwale, B. R. Marathe, V. G. Bhide, J. Mater. Sci. 1992, Vol. 27, 4705.
14. S. Ezhilvalavam, T. R. N. Kutty, Mater. Chem. Phys. 1997, Vol. 49, 258.
15. M. L. de la Olvera, R. Asomoza, Sens. Actuators, 1997, Vol. 45, 49.
16. X. Jiaqiang, C. Yuping, C. Daoyong, S. Jianian, Sens. Actuators B, 2006,113, 526.
17. V. R. Shinde, T. P. Gujar and C. D. Lokhande, Sens. & Actuators B, 2007, 120, 551.
18. M. Law, L. E. Greene, J.C. Hohnson, R. Saykally, P. Yang, Nature, 2005, 4, 455.
19. R. S. Mane, W. J. Lee, H. M. Pathan, S. H. Han, J. Phys. Chem., B, 2005, B 109, 242-54.
20. J. B. Baxter and E. S. Aydil, Solar Energy Mater. Solar Cells, 2006, 90, 607-622.
21. A. Ennaoui, M. Weber, R. Scheer, H.J. Lewerenz, Sol. Energy Mater. Sol. Cells, 1998, 54, 277.
22. J. Liqiang, W. Baiq, X. Baifu, L. Shudan, S. Keying, C. Weimin, F. Honggang, J. Solid State Chem. 2004, 177, 4221.
23. M.H. Huang, S. Mao, H. Feick, H. Yan, Y. Wu, H. Kind, E. Weber, R. Russo, P. Yang, Science,2001 292, 1897.
24. D.C. Reynolds, D.C. Look, B. Jogai, Solid State Commun., 1996, 99,873.
25. R. Das, S. Ray, J. Phys. D: Appl. Phys. 2003, 36, 152.
26. H. Ohno, Science, 1998, 281, 951.
27. G. S. T. Rao, D. T. Rao, Sens. Actuator B, 1999, 55, 166.
28. B. Ismail, M.A. Abaab, B. Rezig, Thin Solid Films, 2001, 383, 92.
29. Joseph Benny, K.G Gopalchandran, P.K.Manoj, Koshy Peter, V.K.Vidyan, Bull. Mater. Sci., 1999, 22, 921.
30. B.D. Cullity, In: “Elements of X-ray diffraction 2nd Edition” Addison Wesley (Publishing co. inco. London, 1978), 102.
31. D. R. Patil, L. A. Patil, IEEE Sensors Journal, 2007, 7[3], 434-439.
32. JCPDS Card Number 21-1486 ZnO (1992).
33. H. Tang, K. Prased, R. Sanjine’s F. Levy, Sens. & Actu. B, 1995, 26- 27, 71-75.
34. S. C. Gadkari, Solid State Physics Symposium, 1998, Kurukshetra Uni. Kurukshetra, 41.
35. Jia Grace Lu, Electrically controlled nanowire-based chemical sensors, SPIE, 8 June 2006.